

DATABASE

Open Access



Creating a digital database of tephra fallout distribution and frequency in Japan

Shimpei Uesawa^{1*}, Kiyoshi Toshida¹, Shingo Takeuchi¹ and Daisuke Miura^{1,2}

Abstract

Tephra fallout is a potential hazard to livelihoods, critical infrastructure, and health, even in areas that are far from volcanoes. Therefore, it is important to quantitatively evaluate tephra fall hazards for both residents and infrastructure around hazardous volcanoes. Modern probabilistic volcanic hazard assessments of tephra fallout strongly rely on computer modeling; however, assessments based on isopach maps can also be helpful in assisting decision-makers. To assess the tephra fall hazards in Japan, we created a digital database “Isopach map-Based Tephra fall Hazard Analysis (IB-THA)” and a tool to draw the cumulative number of tephra fallout events exceeding a specific thickness at a particular location. The database was re-digitized using an existing catalog of 551 tephra fall deposit distribution maps. The re-digitized datasets were utilized here to estimate the cumulative number of tephra fallout events exceeding a specific thickness at 47 prefectural offices for the last 150 kyr. This allowed the characterization of regional tephra fall hazards in Japan for the first time. High cumulative numbers (20) of tephra fall deposits > 0 mm were identified in the NE-E region (e.g., Maebashi), whereas low numbers (2) were recognized in the SW and W regions of Japan (e.g., Naha). The thickest tephra fall deposit (2850 mm) was observed at Kagoshima. We used IB-THA to create a hazard curve for Tokyo. This hazard curve provides the minimum frequency needed to exceed the tephra fall thickness at any location. To refine the digital database presented here, further studies are required to incorporate recent (i.e., 2003 or younger) tephra distributions, review questionable isopach maps, and improve the interpolation method for digitizing tephra fall distributions.

Keywords: Probabilistic tephra fall hazard assessment, Tephra fall thickness, Database, Hazard curve

Introduction

Tephra fallout is a potential hazard to densely populated areas in modern global communities. Tephra fallout may cause roof collapses due to tephra mass load, short circuits due to the adhesion of fine ash particles to insulators (e.g., Wilson et al., 2014), and mechanical failures due to the intrusion and accumulation of ash particles, resulting in the disruption of public transportation services and electricity networks (e.g., Wardman et al., 2012; Blong et al., 2017; Mueller et al., 2020). To plan measures

to mitigate these potential risks, a quantitative assessment of tephra fall hazards and their potential impacts need to be conducted first.

Quantitative tephra fall hazard assessment has been performed using two major approaches: deterministic and probabilistic. Deterministic approaches using eruption scenarios based on historical literature and observation records have been adopted worldwide, particularly for producing volcanic hazard maps (e.g., Waythomas et al., 1998; Nakasuji and Satake, 2004; Becker et al., 2010; Takarada, 2017; Fujita et al., 2019). Probabilistic approaches can be divided into “objective” (e.g., frequentist; Cox and Lewis, 1966) and “subjective” (e.g., expert elicitation; Budnitz et al., 1997). There are two methods of objective probabilistic approach:

*Correspondence: uesawa@criepi.denken.or.jp

¹ Nuclear Risk Research Center, Central Research Institute of Electric Power Industry (CRIEPI), 1646 Abiko, Abiko City, Chiba Pref 270-1194, Japan
Full list of author information is available at the end of the article



© The Author(s) 2022. **Open Access** This article is licensed under a Creative Commons Attribution 4.0 International License, which permits use, sharing, adaptation, distribution and reproduction in any medium or format, as long as you give appropriate credit to the original author(s) and the source, provide a link to the Creative Commons licence, and indicate if changes were made. The images or other third party material in this article are included in the article's Creative Commons licence, unless indicated otherwise in a credit line to the material. If material is not included in the article's Creative Commons licence and your intended use is not permitted by statutory regulation or exceeds the permitted use, you will need to obtain permission directly from the copyright holder. To view a copy of this licence, visit <http://creativecommons.org/licenses/by/4.0/>. The Creative Commons Public Domain Dedication waiver (<http://creativecommons.org/publicdomain/zero/1.0/>) applies to the data made available in this article, unless otherwise stated in a credit line to the data.

1) a stochastic approach and 2) a statistical empirical approach (Marzocchi and Bebbington, 2012). The stochastic approach considers the frequency of eruptions and the distributions of eruption size and wind direction. This approach has been used to simulate, via computer modeling: a) tephra fallout from one volcano on a local scale (e.g. Barberi et al., 1990; Connor et al., 2001; Bonadonna et al., 2005; Bebbington et al., 2008; Costa et al., 2009; Yamano et al., 2018; Mastin et al., 2020); and b) tephra fallout from multiple volcanoes on a regional to global scale (e.g. Yokoyama et al., 1984; Hoblitt et al., 1987; Hurst and Smith, 2004, 2010; Jenkins et al., 2012a; Jenkins et al., 2012b; Bear-Crozier et al., 2016; Miller et al., 2016; Jenkins et al., 2018). The stochastic approach can account for uncertainties stemming from various sources (e.g., simplified physical model of tephra fallout; Suzuki, 1983) and eruption source parameters (e.g., erupted mass, plume dimensions, wind profiles, eruption duration; Bonadonna et al., 2005) through a large number of calculations. The output from such models is a probability curve of exceeding a specific tephra mass load (i.e., hazard curve).

The statistical empirical approach calculates the frequencies of tephra fallout events based on tephra fall records (i.e., tephra fall deposits). This method relies only on the tephra fall record, although a large catalog of tephra fall deposits is required (Marzocchi and Bebbington, 2012). For catalogs we refer to a compilation of well-preserved tephra layers (ideally from several outcrops or drilled borehole cores) (e.g., Cioni et al., 2003; Hurst and Smith, 2004, 2010; Magill et al., 2006).

Herein, we propose a new statistical empirical method based on a large collection of isopach maps produced across Japan. By constructing a raster data set of tephra fallout distribution maps, we determine the frequency of regional tephra fallout, which can be used to refine hazard assessment strategies. We have named the method “Isopach map-Based Tephra fall Hazard Analysis (IB-THA)”.

Firstly, we re-digitized the database of Suto et al. (2007) to obtain the geological record-based number of tephra fallout events. Then, we analyzed it at 47 locations (prefectural offices) to recognize some key regional characteristics, such as frequencies of tephra fall deposits exceeding 0 mm and the maximum thickness of such deposits. Furthermore, we compared tephra fall records with borehole cores at two specific locations where many tephra fall deposits are well preserved. Herein, we also propose a method to illustrate the hazard curve based on the mean annual frequency of exceedance. We believe that this method and its successive iterations will provide a low-cost, empirical

statistical assessment of regional tephra fall hazards in Japan.

Tephra fallout isopach map database in Japan

Isopach maps of tephra fall deposits have been published in Japan over the past 60 years (e.g., Machida, 1964a, 1964b; Hayakawa, 1985; Miyabuchi, 2009; Uesawa et al., 2016). The first systematic compilation of these maps was a pioneering work by Machida and Arai (1992). The revised version was published in 2003 as an atlas of eruptions from ca. 400 ka to AD 2003 in and around Japan (Machida and Arai, 2003). Later, Suto et al. (2007) compiled maps from Machida and Arai (2003) and other sources prior to 2003, digitized them, and then draw isopachs by interpolating thicknesses via geometric techniques. In addition to compiling the isopach map database, Suto et al. (2007) determined the cumulative thickness of tephra fall deposits and obtained the maximum and minimum thicknesses of the expected deposit for each city and town in Japan for the past 1, 10, and 100 kyr. However, their database cannot be directly applied to obtain tephra fall information at an arbitrary locality because the isopachs are provided in a portable document format (PDF) file, so they lack digitized georeferenced data (e.g., shapefile format).

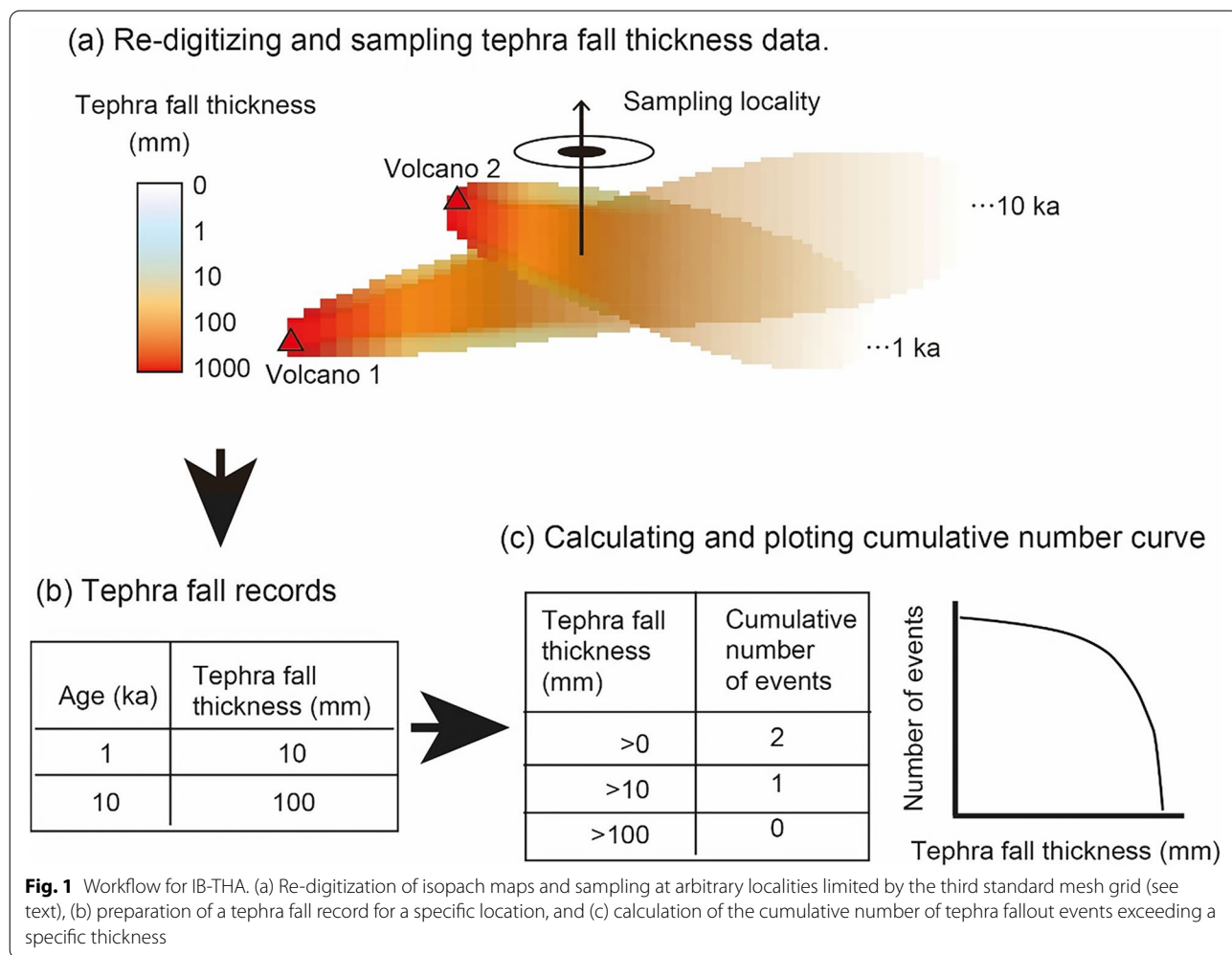
To analyze the tephra fallout events within the catalog of Suto et al. (2007), we georeferenced, and re-digitized their 551 isopach maps by means of geographic information system (GIS) analysis (here we used ArcGIS 10.5). The details of the method are provided in the next section.

Methods

IB-THA (Fig. 1), which includes a dataset of digital tephra distribution maps and a tool to determine the number of tephra fallout events exceeding a specific thickness, was conducted using the procedures presented in this section.

Data preparation

Firstly (Fig. 1a), we georeferenced and digitized the maps (551) from Suto et al. (2007) in GIS to construct a digital database of tephra fall distributions. These digital distribution maps were obtained using the following methods: (1) the original isopach maps were georeferenced; (2) for each map, the isopachs were digitized; (3) each isopach was assigned a specific thickness; and (4) the digitized isopachs were transformed into raster data. The raster dataset is available in Uesawa (2020). The grid size of the raster was defined as the third standard mesh grid (mesh size of 30" latitude and 45" longitude, which equals 1 km × 1 km). The mesh grid was defined following the standards of Ministry of Land, Infrastructure, Transport, and Tourism of Japan.



Forty maps out of the 551 available were not included in our new database for the following reasons. (1) Six maps were not included in the original database of Suto et al. (2007). (2) One record of the Sambe–Uki-nuno tephra (U2, Katoh et al., 1996) was found here to have significant thickness value errors, in addition to being a duplicate of the Suk tephra in Machida and Arai (2003). (3) A duplicate of the 1979 Aso volcano eruption was included in the Hayakawa and Imura (1991) and Ono et al. (1995) databases. (4) In the Older Fuji Volcano (~100 ka) record (Machida, 1964b), Suto et al. (2007) included the thickness of the Kanto Loam layer. We excluded these data because Kanto Loam comprises multiple eruption products derived from the Hakone and Older Fuji volcanoes, as well as aeolian dust deposits (loess; Hayakawa, 1995; Suzuki, 1995). (5) Thirty-one maps showing sub-units were excluded and maps showing the summed (cumulative) thickness of those

sub-units were adopted as representative of each eruption instead. For instance, 3 subunits—Aira Tn-I, Tn-II, and Tn-III (Nagaoka, 1988)—were not included here. Instead, we included the isopach map of “AT” (Machida and Arai, 1992) as a representative tephra fall deposit for the Aira–Tanzawa eruption. All events are listed in Table ST1 in Supplementary Material 1.

Furthermore, the following four eruptions include multiple tephra fall sub-units: Kikai–Akahoya tephra (K-Ah; ~73 ka), Aira–Tanzawa tephra (AT; 26–29 ka), Numazawa caldera (Nm-N; 5 ka), and Suwanose Island (AD 1813) (Shimano and Koyaguchi, 2001). The cumulative thicknesses of the following sub-units were implemented in our dataset: Koya pumice fall for K-Ah; Osumi pumice fall for AT; sub-units IV, III, and II for Nm-N; and units A, B, C–E, F, and G for Suwanose AD 1813. Hence, twelve subunits were summarized into 4 units. After these corrections, the total number of events in our database was 503.

Calculation of tephra fallout records and cumulative number of tephra fallout events exceeding specific thicknesses

The aforementioned re-digitized database was used to calculate the cumulative number of tephra fallout events exceeding a specific thickness curve (Fig. 1c), by implementing the following methods.

For the second step (Fig. 1b), tephra fallout events were counted at arbitrary sampling points limited by the grid. Subsequent tests of tephra fallout events and their respective thicknesses were sampled for all prefectural offices and two specific drilling sites (Lake Suigetsu, Albert et al., 2019, and Uwa basin, Tsuji et al., 2018). The code used for sampling is available at <https://github.com/s-uesawa/Prototype-TephraDB-Japan>.

For the last step (Fig. 1c), cumulative numbers of events exceeding specific tephra fall thicknesses were calculated and graphs were created. Specific thicknesses were 0 mm, 0.1 mm, 1 mm, and 10 mm, the latter ranging from 10

to 3000 mm at 10 mm steps. Suto et al. (2007) reported thicknesses in centimeters; therefore, the accuracy of their tephra fall deposit thicknesses is 10 mm. The interpolation method implemented here allow for thicknesses < 1 mm to be estimated by using our database.

Results

Characteristics of the database

Using the criteria described above, 503 tephra fallout records in our new database were selected to inspect tephra fall hazards in Japan (Fig. 2). We present the results after analyzing the data in terms of the number of events at 10 ka steps for the past 330 kyr, grouped by Volcanic Explosivity Index (VEI: Newhall and Self, 1982) estimated by Suto et al. (2007) (Table 1; Figs. 3 and 4). In addition, the relationship between VEIs and tephra fallout events greater than 0 mm thickness at 47 prefectural offices (Fig. 2), and the examination of the dominant period of tephra fallout events greater than 0 mm

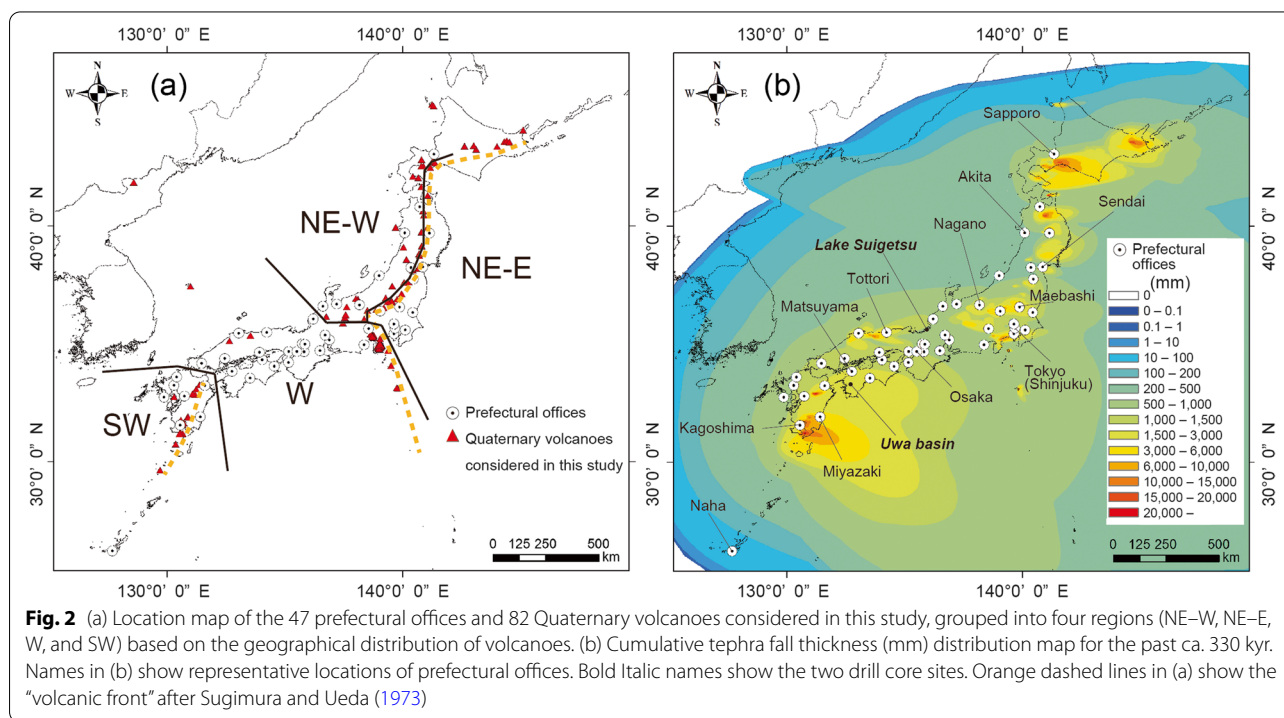
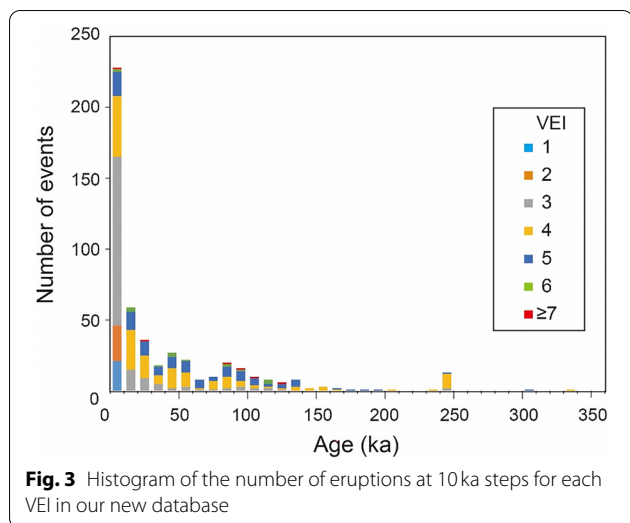


Fig. 2 (a) Location map of the 47 prefectural offices and 82 Quaternary volcanoes considered in this study, grouped into four regions (NE-W, NE-E, W, and SW) based on the geographical distribution of volcanoes. (b) Cumulative tephra fall thickness (mm) distribution map for the past ca. 330 kyr. Names in (b) show representative locations of prefectural offices. Bold italic names show the two drill core sites. Orange dashed lines in (a) show the "volcanic front" after Sugimura and Ueda (1973)

Table 1 Number of eruptive events for different VEI and time periods. VEIs estimated by Suto et al. (2007)

VEI	1	2	3	4	5	6	≥7	Total
Holocene (younger than 10 ka)	21	25	121	47	18	2	1	235
Younger than 50 ka	21	25	152	112	60	9	2	381
Younger than 100 ka	21	25	161	137	87	13	4	448
Younger than 150 ka	21	25	165	148	100	16	6	481
Total number of events	21	25	167	162	106	16	6	503



thickness at 47 prefectural offices, are shown in Figs. 5 and 6.

The size of our dataset is smaller than that used by Kiyosugi et al. (2015), which are 700 eruption records, because tephra fallout events lacking distribution maps were not included in our study. The frequency of eruption events declines with increasing age for all VEI values (Fig. 3). This is the case for both the Japanese and global databases (e.g., Deligne et al., 2010; Kiyosugi et al., 2015; Nakada, 2015; Bear-Crozier et al., 2016), and it was also observed by Suto et al. (2007). This may have been caused by the under-recording of eruptions in the pre-historic era and a lack of preservation, as suggested by Kiyosugi et al. (2015). Generally, the number of smaller VEI events geologically observed rapidly decreases with an increase in eruption age. For instance, all the VEI 1–2 events

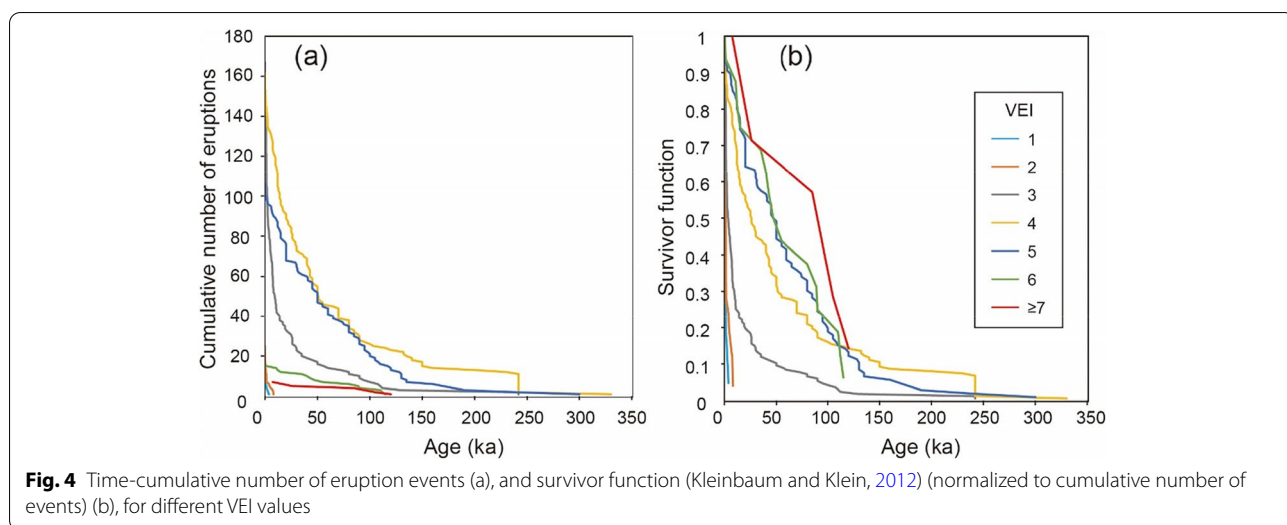
and ~73% of the VEI 3 events were recorded during the Holocene (Figs. 3 and 4; Table 1).

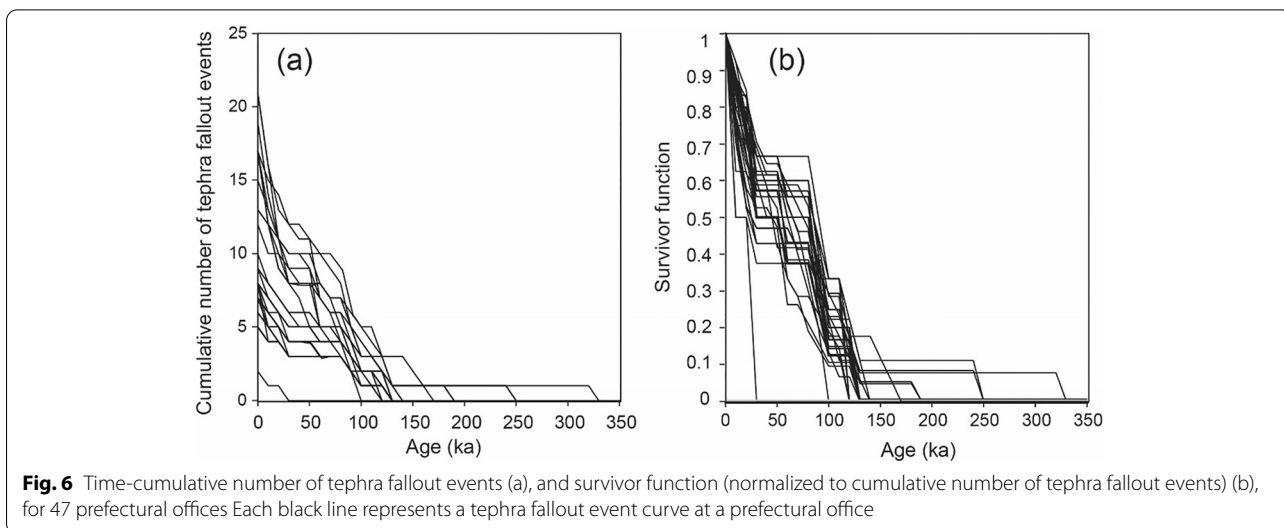
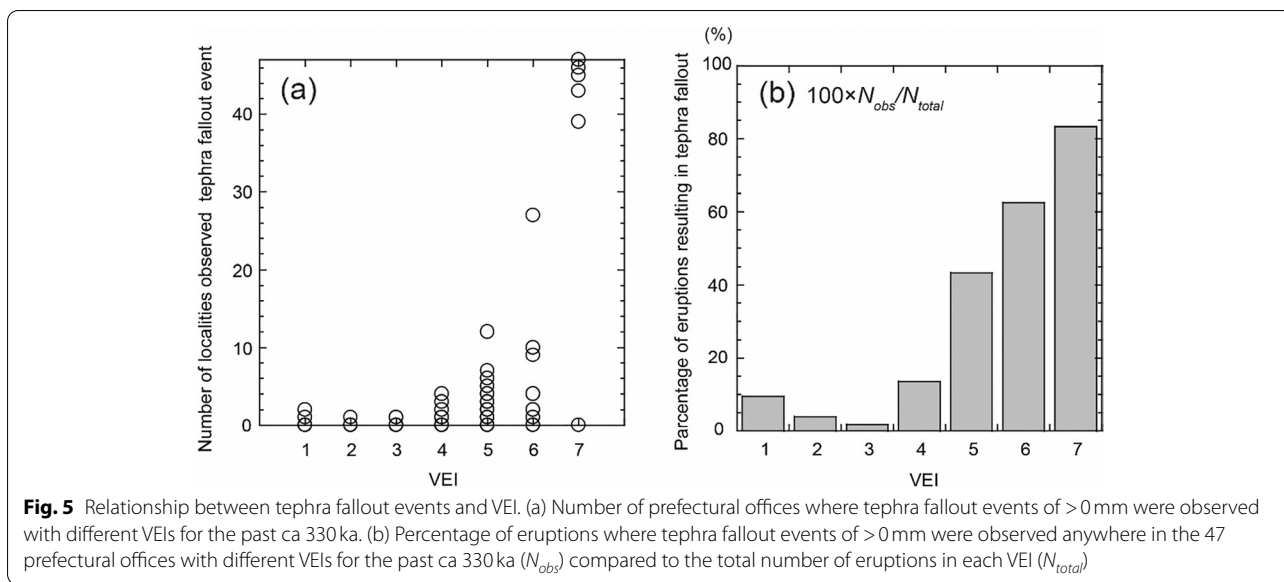
The cumulative number of tephra fallout events over time, and the corresponding survivor function (Kleinbaum and Klein, 2012) (normalized to the cumulative number of tephra fallout events) at 47 prefectural offices, based on an evaluation of tephra fall deposits >0 mm, are shown in Fig. 6. Most exhibit a linear decrease with an increase in age over the last 150 kyr. This suggests that tephra fallout events >0 mm occurred constantly during this time interval. Approximately 90% of the recorded events for every prefectural office occurred over the last 150 kyr. Therefore, we used a subset of eruptive events younger than 150 ka for the subsequent analysis.

Cumulative number of tephra fallout events exceeding a specific thickness during the last 150 kyr at 47 prefectural offices

The number of tephra fallout events exceeding a specific thickness for the last 150 kyr at 47 prefectural offices was calculated using IB-THA. Here, we describe the patterns of the number of tephra fallout events exceeding a specific thickness at specific key locations. The corresponding graphs are shown in Fig. 7.

In general, the localities with a relatively low cumulative number of thicker events do not vary considerably with an exceeding specific thickness (Fig. 7b, ii to iv), whereas those with a higher cumulative number of thinner events do vary (Fig. 7b, i). Cumulative number of events higher than 10 for thicknesses > 0 mm are recognized in every region of Japan. Especially in NE–E Japan (see Figs. 7b-i and 8a), located to the east of the central to northeastern volcanic zone. Regions that have experienced tephra fallout



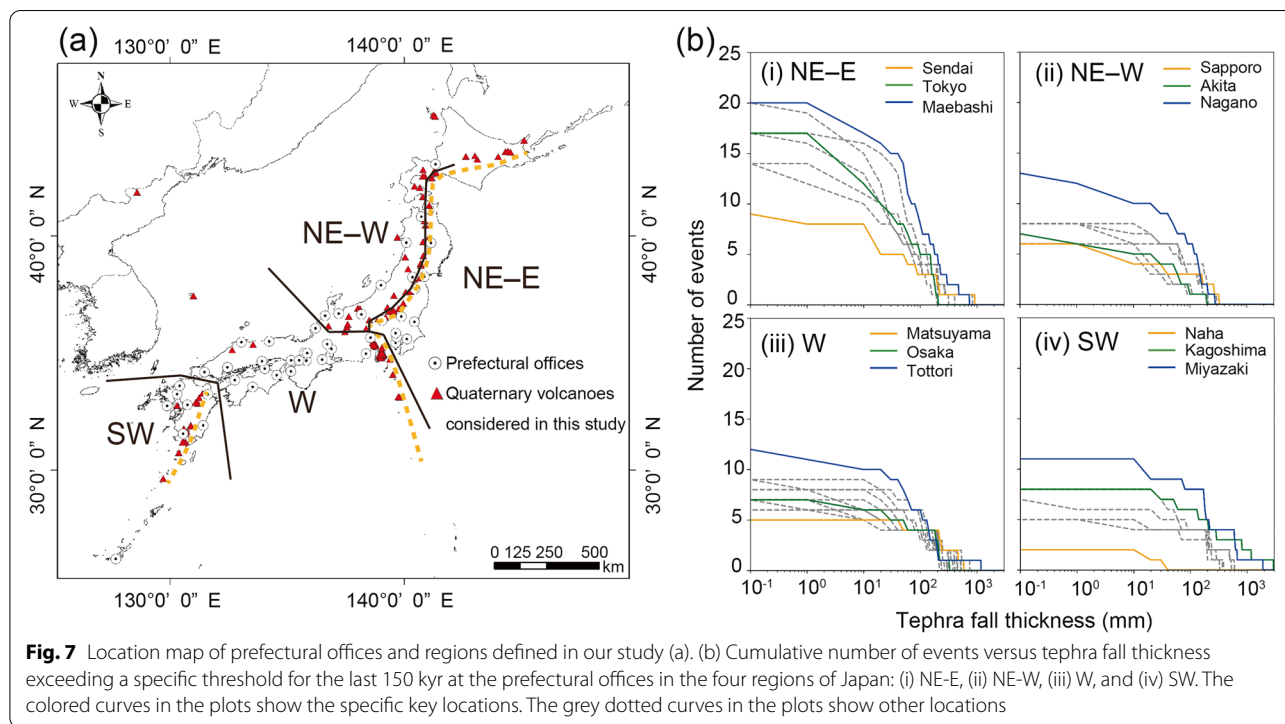


events with thickness >1000 mm are recognized in SW and W Japan (e.g., Kagoshima, Tottori, Fig. 7b, iii-iv; Fig. 8b). The most common thicknesses for the 47 prefectural offices ranged from 200 to 300 mm (Fig. 8b).

Discussion
Evaluation of regional characteristics of tephra fall hazard in Japan

The cumulative number of tephra fallout events over the last 150 kyr can be used to analyze the characteristics of the tephra fall hazards in Japan. These characteristics are dependent on the relationships between the locations of the sampling points and the locations of the volcanoes that produce tephra fallout.

For instance, the high cumulative number of tephra fallout events represented in the NE-E region (Figs. 7 and 8a) indicates tephra sourced from many volcanoes in Japan, which includes proximal volcanoes, and even distant calderas in the SW region. Tephra sourced from caldera-forming eruptions can be dispersed over long distances (500–1000 km) by westerly stratospheric winds in Japan. The cumulative number of tephra fallout events are similar for the SW, W, and NW-E regions (Figs. 7 and 8a) because many large tephra-producing eruptions occurred in the SW region. In fact, the thickest tephra fall deposits were observed in the SW region because caldera-forming eruptions occurred close to the cities considered in this study in that region (e.g., Kyushu Island). For the rest of the prefectural



offices, the maximum thicknesses range from 100 to 1000 mm (Fig. 8b).

Comparison of the database with drill core data

Well preserved drill core datasets with precise carbon dating have been obtained for tephra fall deposits and fluvio-lacustrine sediments in Japan (e.g., Tsuji et al., 2018; Albert et al., 2019). We compared two such drill core datasets with our database at the same locations using the cumulative number of tephra fall thicknesses for the last 150 kyr. The localities chosen for the calculations were Lake Suigetsu (Suigetsu SG06 drill core, <135 ka; Albert et al., 2019) and the Uwa basin (UT drill core, <600 ka; Tsuji et al., 2018) (Figs. 2b and 9). Those two sites were chosen because they contain the best-preserved deposits and are well documented for accurate tephra correlation (e.g., thicknesses, compositions, ages) published in the literature.

A comparison of drill core SG06 with our database (Fig. 9a) revealed two differences: (1) the core displays a higher cumulative number of tephra fall thicknesses >0mm (Fig. 9, green lines) compared with that of the database (Fig. 9, orange lines); and (2) there is a slight discrepancy in the thickest event documented in the core (Fig. 9, green lines) and that in the database (Fig. 9, orange lines). The lower cumulative number of tephra fall thicknesses exceeding 0mm in the database may be

due to: (1) a lack of preservation of some tephra fall-out events (e.g., thin tephra fall deposits derived from small-magnitude eruptions or distal thin deposits from large events), or (2) a lack of isopach maps (e.g., unpublished data or tephra thicknesses only reported at a few localities, so the distribution of the deposit has not been determined). The small discrepancies between the events with greater tephra thicknesses may be attributed to the interpolation method of Suto et al. (2007) and that used here for the new database, or to erosion and/or compaction of the drill core deposits. We assumed that compaction was due to weathering of the tephra fall deposit and loading by subsequent deposits. For example, fresh thin tephra fall deposit densities range from 230 to 1600 kg/m³ (e.g., Blong et al., 2017; Osman et al., 2022), whereas compacted thin tephra fall deposit densities range from approximately 1300 to 1800 kg/m³ (Blong et al., 2017). Weathered compacted tephra fall deposits are considered to have densities of up to 2500 kg/m³ (e.g., Wohletz and Heiken, 1992). Thus, tephra fall deposit thicknesses reported in literature may include some uncertainty. Although the database has limitations (interpolation of isopach maps, preservation degree of tephra fall deposits), comparisons with borehole data suggest that the database can be useful for evaluating tephra fall hazards, especially for large-magnitude eruptions and/or eruptions affecting several regions.

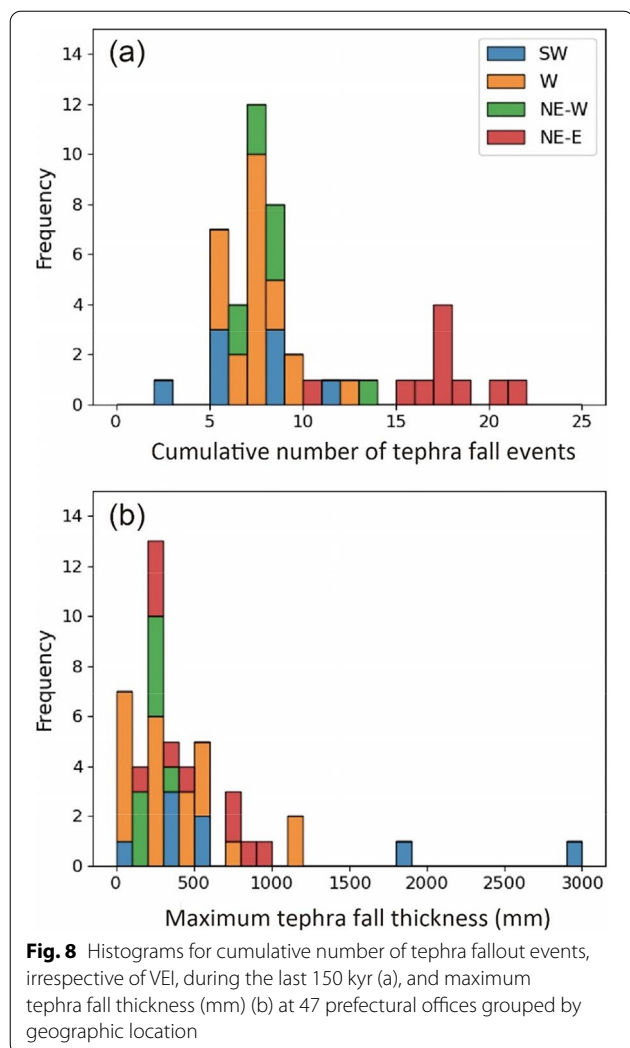


Fig. 8 Histograms for cumulative number of tephra fallout events, irrespective of VEI, during the last 150 kyr (a), and maximum tephra fall thickness (mm) (b) at 47 prefectural offices grouped by geographic location

Proposal of an isopach map-based hazard curve

Hazard curves are useful for evaluating hazards during the risk assessment of artificial objects (e.g., INTERNATIONAL ATOMIC ENERGY AGENCY, 2016). Here, we propose a hazard curve based on the mean annual frequency of exceedance using IB-THA with the following calculations.

The mean annual frequency of exceedance (λ_{an}) for a specific tephra fall thickness t (in mm) at a specific location was calculated as:

$$\lambda_{an} = \frac{N}{T} \tag{1}$$

where N is the number of tephra fallout events exceeding a specific thickness for a specific time interval T (in years).

Here, $1/\lambda_{an}$ denotes the mean return period. To display the mean annual frequency for different exceeding specific thicknesses and for different time intervals, the frequencies (λ_{an}) were calculated at 10 kyr time intervals for the last 150 kyr. Table 2 shows an example of the mean annual frequencies of exceedance in Tokyo for representative tephra fall thicknesses. We observe that the mean annual frequencies in Table 2 mostly decrease with extended periods. This implies that the number of recorded events decreases with time. Therefore, the variations are shown with the 95% confidence interval using the t -distribution (e.g., Altman et al., 2013) (Table 2). Finally, the hazard curve was obtained by incorporating the tephra fall deposit thickness in the horizontal axis and λ_{an} in the vertical axis (Fig. 10). It needs to be emphasized, however, that this hazard curve represents the minimum annual frequency of tephra fall events, because the database excludes the tephra fall deposits that may have been eroded or not reported yet. Furthermore, to

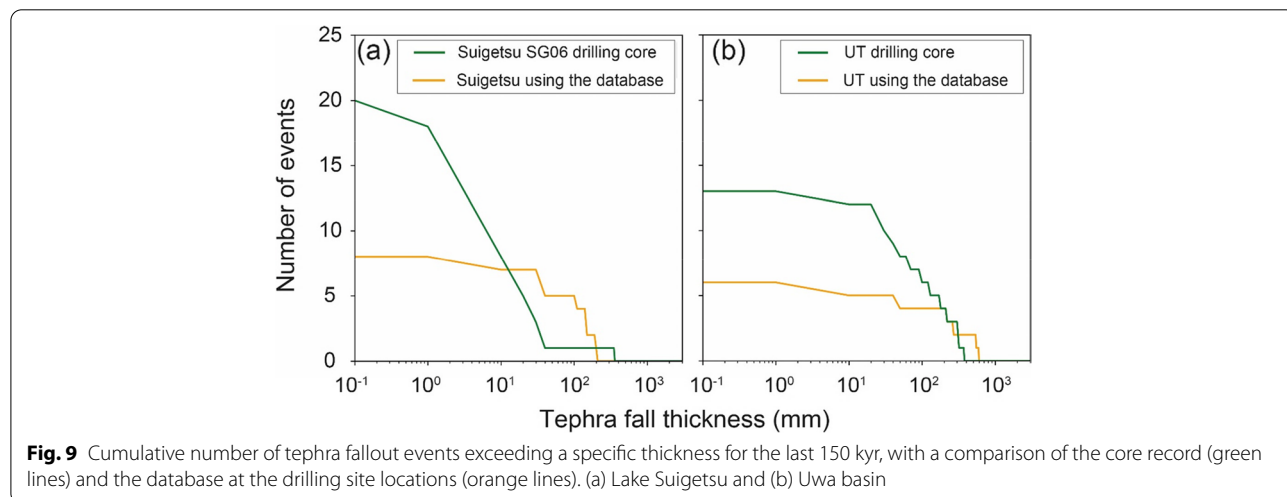
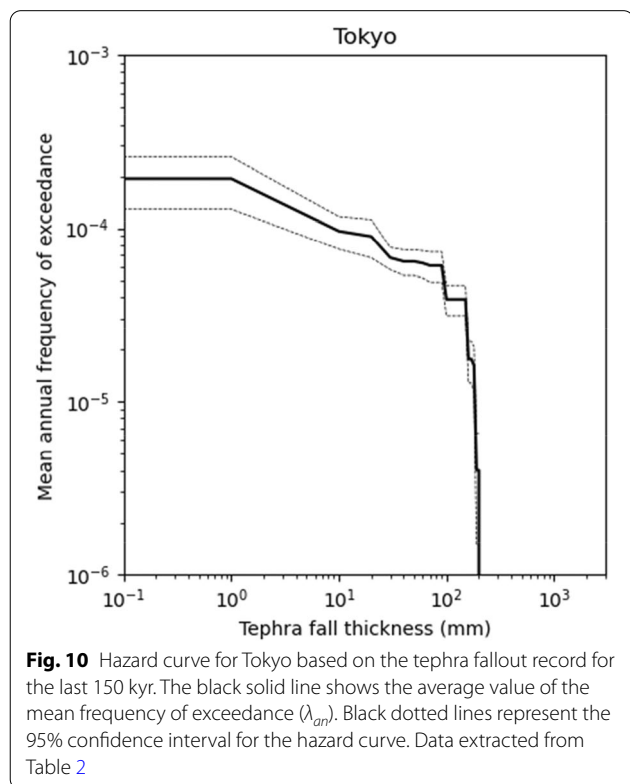


Fig. 9 Cumulative number of tephra fallout events exceeding a specific thickness for the last 150 kyr, with a comparison of the core record (green lines) and the database at the drilling site locations (orange lines). (a) Lake Suigetsu and (b) Uwa basin

Table 2 Variation in the mean annual frequency of tephra fall (λ_{ann}) events exceeding 0 mm and equal to or greater than 10, 100, 200, and 500 mm for every 10 kyr period extended from present to 150 kyr at Tokyo. t : tephra fall deposit thickness (mm); Conf_95_max and Conf_95_min: maximum and minimum values of the 95% confidence interval, respectively. ND: not defined

Age (ka)	$t > 0 (\times 10^{-4})$	$t \geq 10 (\times 10^{-4})$	$t \geq 100 (\times 10^{-4})$	$t \geq 200 (\times 10^{-4})$	$t \geq 500 (\times 10^{-4})$
0–10	5.00	3.00	0.00	0.00	0.00
0–20	4.00	2.00	0.50	0.00	0.00
0–30	3.00	1.67	0.67	0.00	0.00
0–40	2.25	1.25	0.50	0.00	0.00
0–50	1.80	1.00	0.40	0.00	0.00
0–60	1.50	0.83	0.33	0.00	0.00
0–70	1.43	0.86	0.43	0.00	0.00
0–80	1.25	0.75	0.38	0.00	0.00
0–90	1.33	0.89	0.44	0.11	0.00
0–100	1.30	0.90	0.40	0.10	0.00
0–110	1.27	0.91	0.36	0.09	0.00
0–120	1.25	0.92	0.33	0.08	0.00
0–130	1.31	1.00	0.38	0.08	0.00
0–140	1.21	0.93	0.36	0.07	0.00
0–150	1.13	0.87	0.33	0.07	0.00
Mean	1.94	1.18	0.39	0.04	0.00
Conf_95_max	2.58	1.52	0.47	0.07	ND
Conf_95_min	1.29	0.85	0.31	0.02	ND



obtain the tephra fall load it is necessary to convert the thickness data into loads using various deposit densities (e.g., Blong et al., 2017).

Future work

The database generated by Suto et al. (2007) can be improved in several ways:

- (i) Firstly, the data consist of tephra distribution maps for the period between ca. 330ka and AD 2003. Therefore, isopach data for more recent eruptions (e.g., Asama 2004 eruption; Yoshimoto et al., 2005; Kirishimayama–Shinmoedake 2011 eruption; Maeno et al., 2014; Ontake 2014 eruption; Takarada et al., 2016) should also be included.
- (ii) Secondly, some records in the database (e.g., Yotei tephra, SW Hokkaido; Kashiwabara et al., 1976) should be refined to integrate recent revisions (e.g., Uesawa et al., 2016; Tsuji et al., 2018; Albert et al., 2019).
- (iii) There are numerous problems associated with the interpolation methods. For example, the geometric method used to reproduce the isopachs of Suto et al. (2007) includes imprecisions caused by isotopic and/or isometric extensions of isopach lines. The ArcGIS-based interpolation tool implemented

here is widely used in hydrology, but its application for tephra fall deposits is yet to be well tested. Therefore, volcanological methods able to systematically and confidently reproduce and interpolate tephra fall distributions should be tested in future applications. For instance, stochastic empirical methods (e.g., Kawabata et al., 2013; Green et al., 2016; Yang and Bursik, 2016) and inversion algorithms based on the advection–diffusion equations (e.g., Mannen, 2014; Yang et al., 2021) have been successfully applied to reproduce and interpolate tephra fall deposit distributions.

Taking into account these areas of potential future improvements, the method presented here can be utilized to evaluate the distribution of tephra fall hazards. This is particularly useful for sites where tephra deposits are eroded, or for remote, isolated sites where tephra sampling is difficult. Using the method developed in this study, a better view of the distribution of tephra fall deposits in urbanized, highly vegetated, mountainous, and offshore areas can be obtained.

Continuous improvements in the database will lead to a better understanding of the explosive eruption record and tephra distribution patterns in Japan. This information can be used to develop better mitigation measures for the impacts of tephra fall on critical infrastructure and facilities, as well as its effects on human health, agriculture, and other activities (e.g., Wilson et al., 2014; Yamamoto and Nakada, 2014).

Conclusions

We created a digital geospatial database to evaluate tephra fall hazards in Japan (IB-THA). Our main findings are:

- 1) VEI 3–7 explosive eruptions dominate in our database for the < 150 ka period. Smaller (VEI < 3) events may be missing from our record because of erosion.
- 2) Our database enabled us to evaluate tephra fall hazards for various localities in Japan. The cumulative number of tephra fallout events calculated for 47 prefectural offices indicates regional variations in tephra fall distributions and characteristics.
- 3) There were two major differences between the cumulative number of tephra fallout events from the drill core data and those from the digitized tephra database. The first was a significantly smaller number of high-frequency events in the tephra database compared to the drill core data (e.g., 8 versus 20 at the Suigetsu SG06 drill core for > 0 mm thick tephra deposits), which can be explained due to the lack of records for smaller tephra fallout events in the database. The second was a minor difference in the thick-

ness of the thickest tephra fall deposits when our database was compared to the drill core data. This difference might be due to the coarse interpolation methodology used by Suto et al. (2007), and erosion and/or compaction of the drill core deposits.

- 4) Our database can be used to generate a hazard curve for any specific location by using IB-THA. For example, in Tokyo, the mean annual frequency of exceedance is $\sim 1.18 \times 10^{-4}$ for 10 mm thickness tephra fallout.
- 5) The current database is incomplete as it includes events only prior to AD 2003. We therefore suggest the inclusion of more recent explosive eruptions with the aim of refining future analyses for shorter time periods and/or thinner fallout thicknesses.
- 6) Well-tested computer-based interpolation methods (e.g., inversion analyses using the advection–diffusion model, statistical empirical approaches) should be more frequently conducted for tephra fall deposits in Japan. This will help refine the distribution of some tephra fallout events, especially of those with very uncertain hand drawn isopachs.

Abbreviations

IB-THA: Isopach map-Based Tephra fall Hazard Assessment; GIS: Geographic Information System; GMT: Generic Mapping Tool; VEI: Volcanic Explosivity Index..

Glossary

Shapefile	A shapefile is a digital format that stores nontopological geometry and attributes information (in an attribute table) for the spatial features in a dataset. The geometry of a feature is stored in a shape comprising a set of vector coordinates. Shapefiles can support point, line, and area features, such as polygons (ESRI, 1998).
Raster	A raster consists of a matrix of cells (or pixels) organized into rows and columns (a grid), wherein each cell contains a value that represents a specific attribute (e.g., thickness, temperature). Rasters are images that include digital aerial photographs, satellite imagery, digital pictures, or even scanned maps (ESRI, 2016).

Supplementary Information

The online version contains supplementary material available at <https://doi.org/10.1186/s13617-022-00126-x>.

Additional file 1.

Acknowledgments

We are grateful to ESRI Japan and Dr. H Sasaki (Asia Air Survey Co. Ltd.) for their advice on the use of ArcGIS. We also thank Dr. Y Aoyagi (CRIEPI) for help with the Generic Mapping Tool. We appreciate the feedback from Dr. K. Kiyosugi (Kobe University), Dr. K. Mannen (HSRI of Kanagawa Pref.), Dr. S. Jenkins (EOS), Associate Editor D. Bertin and four anonymous reviewers.

Authors' contributions

SU conceived the study, compiled the data, conducted the data analysis, and drafted the manuscript. TK provided advice on the analytical concept and helped draft the manuscript. TS helped collect the original papers (including isopach maps) and provided feedback on the draft manuscript. DM conceived the study together with SU and provided feedback on the draft manuscript. All authors read and approved the final manuscript.

Authors' information

Not applicable.

Funding

All the work for this article was funded by CRIEPI.

Availability of data and materials

The source code for sampling the tephra fall record at an arbitrary locality, and the cumulative number of tephra fallout events exceeding a specific thickness are available at <https://github.com/s-uesawa/Prototype-TephraDB-Japan>. Source code written in R and Python. The raster tephra distribution dataset is available at <https://doi.org/10.5281/zenodo.5109160> in the Tephra_DB_Prototype_ver1.1 folder.

Declarations**Ethics approval and consent to participate**

Not applicable.

Consent for publication

Not applicable.

Competing interests

The authors declare that they have no competing interests.

Author details

¹Nuclear Risk Research Center, Central Research Institute of Electric Power Industry (CRIEPI), 1646 Abiko, Abiko City, Chiba Pref 270-1194, Japan. ²Graduate School of Science, Osaka Metropolitan University, 1-1 Gakuen-Cho, Naka-Ku, Sakai, Osaka 599-8531, Japan.

Received: 19 May 2022 Accepted: 13 November 2022

Published online: 28 November 2022

References

- Albert PG, Smith VC, Suzuki T, McLean D, Tomlinson EL, Miyabuchi Y, Kitaba I, Mark DF, Moriwaki H, SG06 project members, Nakagawa T (2019) Geochemical characterization of the Late Quaternary widespread Japanese tephrostratigraphic markers and correlations to the Lake Suigetsu sedimentary archive (SG06 core). *Quat Geochronol* 52:103–131. <https://doi.org/10.1016/j.quageo.2019.01.005>
- Altman D, Machin D, Bryant T, Gardner M (2013) *Statics with confidence: Confidence intervals and statistical guidelines*, 2nd edn. BMJ Books, Wiley, Hoboken, p 254 ISBN: 978-1-118-70250-5
- Barberi F, Macedonio G, Pareschi MT, Santacroce R (1990) Mapping the tephra fallout risk: an example from Vesuvius, Italy. *Nature* 344:142–144
- Bear-Crozier AN, Miller V, Newey V, Horspool N, Weber R (2016) Probabilistic volcanic ash hazard analysis (PVAHA) I: development of the VAPAH tool for emulating multi-scale volcanic ash fall analysis. *J Appl Volcanol* 53. <https://doi.org/10.1186/s13617-016-0043-4>
- Bebbington M, Cronin SJ, Chapman I, Turner MB (2008) Quantifying volcanic ash fall hazard to electricity infrastructure. *J Volcanol Geotherm Res* 177:1055–1062. <https://doi.org/10.1016/j.jvolgeores.2008.07.023>
- Becker J, Saunders WSA, Robertson CM, Leonard GS, Johnston DM (2010) A synthesis of challenges and opportunities for reducing volcanic risk through land use planning in New Zealand. *Aust J Disaster Trauma Stud* 2010-1. ISSN: 1174-4707 2010-1. <https://www.massey.ac.nz/~trauma/issues/2010-1/becker.htm>
- Blong RJ, Grasso P, Jenkins SF, Magill CR, Wilson TM, McMullan K, Kandlbauer J (2017) Estimating building vulnerability to volcanic ash fall for insurance and other purposes. *J Appl Volcanol* 6:2. <https://doi.org/10.1186/s13617-017-0054-9>
- Bonadonna C, Connor CB, Houghton BF, Connor L, Byrne M, Laing A, Hincks TK (2005) Probabilistic modeling of tephra dispersal: Hazard assessment of a multiphase rhyolitic eruption at Tarawera. *New Zealand J Geophys Res* 110:B03203. <https://doi.org/10.1029/2003jb002896>
- Budnitz RJ, Apostolakis G, Boore DM, Cluff LS, Coppersmith KJ, Cornell CA, Morris PA (1997) Senior Seismic Hazard Analysis Committee; Recommendations for probabilistic seismic hazard analysis: Guidance on uncertainty and use of experts, vol 1–2. U.S. Nuclear Regulatory Commission, U.S. Dept. of Energy, Electric Power Research Institute NUREG/CR-6372, UCRL-ID-122160
- Cioni R, Longo A, Macedonio G, Santacroce R, Sbrana A, Sulpizio R, Andronico D (2003) Assessing pyroclastic fall hazard through field data and numerical simulations: example from Vesuvius. *J Geophys Res* 108(2063):B2. <https://doi.org/10.1029/2001JB000642>
- Connor CB, Hill BE, Winfrey B, Franklin NM, La Femina PCL (2001) Estimation of volcanic hazards from tephra fallout. *Nat Hazards Rev* 2:33–42. [https://doi.org/10.1061/\(ASCE\)1527-6988\(2001\)2:1\(33\)](https://doi.org/10.1061/(ASCE)1527-6988(2001)2:1(33))
- Costa A, Dell'Erba F, Di Vito MA, Isaia R, Macedonio G, Orsi G, Pfeiffer T (2009) Tephra fallout hazard assessment at the Campi Flegrei caldera (Italy). *Bull Volcanol* 71:259–273. <https://doi.org/10.1007/s00445-008-0220-3>
- Cox DR, Lewis PAW (1966) *The statistical analysis of series of events*. Methuen's Monographs on Applied Probability and Statistics, London <https://link.springer.com/book/9789401178037>
- Deligne NI, Coles SG, Sparks RSJ (2010) Recurrence rates of large explosive volcanic eruptions. *J Geophys Res* 115:B06203. <https://doi.org/10.1029/2009JB006554>
- ESRI (1998) ESRI shapefile technical description. An ESRI white paper J-7855 p26. <https://www.esri.com/library/whitepapers/pdfs/shapefile.pdf>
- ESRI (2016) What is a raster data? <https://desktop.arcgis.com/ja/arcmap/10.3/manage-data/raster-and-images/what-is-raster-data.htm>
- Fujita E, Iriyama Y, Shimbori T, Sato E, Ishii K, Suzuki Y, Tsunematsu K, Kiyosugi K (2019) Evaluating volcanic hazard risk through numerical simulations. *J Disaster Res* 14:604–615. <https://doi.org/10.20965/jdr.2019.p0604>
- Green RM, Bebbington MS, Jones G, Cronin SJ, Turner MB (2016) Estimation of tephra volumes from sparse and incompletely observed deposit thicknesses. *Bull Volcanol* 78:25. <https://doi.org/10.1007/s00445-016-1016-5>
- Hayakawa Y (1985) Pyroclastic geology of Towada volcano. *Bull Earthq Res Inst Univ Tokyo* 60:507–592
- Hayakawa Y (1995) Characteristics of Japanese loam, and its eolian origin. *Bull Volcanol Soc Jpn* 40:177–190 (in Japanese with English abstract). https://doi.org/10.18940/kazan.40.3_177
- Hayakawa Y, Imura R (1991) Eruptive history of the past 80,000 years of Aso volcano and the 1989 eruption. *Bull Volcanol Soc Jpn* 36:25–35. https://doi.org/10.18940/kazan.36.1_25
- Hurst T, Smith W (2004) A Monte Carlo methodology for modelling ashfall hazards. *J Volcanol Geotherm Res* 138:393–403. <https://doi.org/10.1016/j.jvolgeores.2004.08.001>
- Hurst T, Smith W (2010) Volcanic ashfall in New Zealand – probabilistic hazard modelling for multiple sources. *N Z J Geol Geophys* 53:1–14. <https://doi.org/10.1080/00288301003631129>
- INTERNATIONAL ATOMIC ENERGY AGENCY (2016) Volcanic Hazard assessments for nuclear installations: methods and examples in site evaluation, IAEA-TECDOC-1795. IAEA, Vienna <https://www.iaea.org/publications/11063/volcanic-hazard-assessments-for-nuclear-installations-methods-and-examples-in-site-evaluation>
- Jenkins S, Magill C, McAneney J, Blong R (2012a) Regional ash fall hazard I: A probabilistic assessment methodology. *Bull Volcanol* 74:1699–1712. <https://doi.org/10.1007/s00445-012-0627-8>
- Jenkins S, McAneney J, Magill C, Blong R (2012b) Regional ash fall hazard II: Asia–Pacific modelling results and implications. *Bull Volcanol* 74:1713–1727. <https://doi.org/10.1007/s00445-012-0628-7>
- Jenkins SF, Magill CR, Blong RJ (2018) Evaluating relative tephra fall hazard and risk in the Asia–Pacific region. *Geosphere* 14:492–509. <https://doi.org/10.1130/ges01549.1>
- Kashiwabara M, Hirose Y, Kagawa M, Kan K, Kasugai A, Yamagishi K (1976) The tephra of Yotei volcano Daiyoni-kenkyu 15:75–86 (in Japanese with English abstract)
- Katoh S, Danhara T, Yamashita T, Takemura K, Okada A (1996) Late Quaternary tephra layer derived from Samba volcano discovered in Kobe City, western Japan. *Daiyoni-kenkyu* 35:383–389 (in Japanese with English abstract)
- Kawabata E, Bebbington MS, Cronin SJ, Wang T (2013) Modeling thickness variability in tephra deposition. *Bull Volcanol* 75:738. <https://doi.org/10.1007/s00445-013-0738-x>
- Kiyosugi K, Connor C, Sparks RSJ, Crowther HS, Brown SK, Siebert L, Wang T, Takarada S (2015) How many explosive eruptions are missing from the geologic record? Analysis of the quaternary record of large magnitude

- explosive eruptions in Japan. *J Appl Volcanol* 4:17. <https://doi.org/10.1186/s13617-015-0035-9>
- Kleinbaum DG, Klein M (2012) *Survival analysis: a self-learning text*, Third edn. Springer, p 700. <https://doi.org/10.1007/978-1-4419-6646-9>
- Machida H (1964a) Tephrochronological study of volcano Fuji and adjacent areas (part 1). *J Geogr (Chigaku Zasshi)* 73:293–308 (in Japanese with English abstract). <https://doi.org/10.5026/jgeography.73.293>
- Machida H (1964b) Tephrochronological study of volcano Fuji and adjacent areas (part 2). *J Geogr (Chigaku Zasshi)* 73:337–350 (in Japanese). <https://doi.org/10.5026/jgeography.73.337>
- Machida H, Arai F (1992) *Atlas of tephra in and around Japan*. University of Tokyo Press, Tokyo, p 276 (in Japanese)
- Machida H, Arai F (2003) *Atlas of tephra in and around Japan*, (revised edition). University of Tokyo Press, Tokyo, p 336 (in Japanese)
- Maeno F, Nagai M, Nakada S, Burden RE, Engwell S, Suzuki Y, Kaneko T (2014) Constraining tephra dispersion and deposition from three subplinian explosions in 2011 at Shinmoedake volcano, Kyushu. *Japan Bull Volcanol* 76:823. <https://doi.org/10.1007/s00445-014-0823-9>
- Magill CR, Hurst AW, Hunter LJ, Blong RJ (2006) Probabilistic tephra fall simulation for the Auckland region, New Zealand. *J Volcanol Geotherm Res* 153:370–386. <https://doi.org/10.1016/j.jvolgeores.2005.12.002>
- Mannen K (2014) Particle segregation of an eruption plume as revealed by a comprehensive analysis of tephra dispersal: theory and application. *J Volcanol Geotherm Res* 284:61–78. <https://doi.org/10.1016/j.jvolgeores.2014.07.009>
- Marzocchi W, Bebbington MS (2012) Probabilistic eruption forecasting at short and long time scales. *Bull Volcanol* 74:1777–1805. <https://doi.org/10.1007/s00445-012-0633-x>
- Mastin LG, Van Eaton A, Schwaiger HF (2020) A probabilistic assessment of tephra-fall hazards at Hanford, Washington, from a future eruption of mount St. Helens. *Open File Rep. US Department of the Interior, US Geological Survey*, pp 2020–1133
- Miller V, Bear-Crozier AN, Newey V, Horspool N, Weber R (2016) Probabilistic Volcanic Ash Hazard Analysis (PVAHA) II: Assessment of the Asia–Pacific region using VAPAH. *J Appl Volcanol* 5:4. <https://doi.org/10.1186/s13617-016-0044-3>
- Miyabuchi Y (2009) A 90,000-year tephrostratigraphic framework of Aso volcano, Japan. *Sediment Geol* 220:169–189. <https://doi.org/10.1016/j.sedgeo.2009.04.018>
- Mueller W, Cowie H, Horwell CJ, Hurler F, Baxter PJ (2020) Health impact assessment of volcanic ash inhalation: a comparison with outdoor air pollution methods. *GeoHealth* 4:e2020GH000256. <https://doi.org/10.1029/2020GH000256>
- Nagaoka S (1988) The late Quaternary tephra layers from the caldera volcanoes in and around Kagoshima Bay, southern Kyushu, Japan. *Geogr Rep Tokyo Metropol Univ* 23:49–122. https://tokyo-metro-u.repo.nii.ac.jp/?action=pages_view_main&active_action=repository_view_main_item_detail&item_id=2850&item_no=1&page_id=30&block_id=164
- Nakada S (2015) Regularity of volcanic eruptions in terms of volcanic Explosivity index (VEI). *Bull Volcanol Soc Jpn* 60:143–150 (in Japanese with English abstract)
- Nakasuji A, Satake J (2004) Volcanic Hazard map: an introduction and overseas cases. *J Jpn Soc Eng Geol* 44:341–348. <https://doi.org/10.5110/jjseg.44.341>
- Newhall CG, Self S (1982) The volcanic explosivity index (VEI) an estimate of explosive magnitude for historical volcanism. *J Geophys Res* 87:C21231–C21238. <https://doi.org/10.1029/jc087ic02p01231>
- Ono K, Watanabe K, Hoshizumi H, Takada H, Ikebe S (1995) Ash eruption of Nakadake volcano, Aso caldera, and its products. *Bull Volcanol Soc Jpn* 40:133–151. https://doi.org/10.18940/kazan.40.3_133
- Osman S, Thomas M, Crummy J, Carver S (2022) Investigation of geomechanical properties of tephra relevant to roof loading for application in vulnerability analyses. *J Appl Volcanol* 11:9. <https://doi.org/10.1186/s13617-022-00121-2>
- Shimano T, Koyaguchi T (2001) Eruption styles and degassing process of ascending magma of the 1813 eruption of Suwanose-jima volcano, Southwest Japan. *Bull Volcanol Soc Jpn* 46:53–70 (in Japanese with English abstract)
- Sugimura A, Ueda S (1973) *Island arcs: Japan and its environs*. Elsevier:247
- Suto S, Inomata T, Sasaki H, Mukoyama S (2007) Data base of the volcanic ash fall distribution map of Japan. *Bull Geol Surv Japan* 58:261–321 (in Japanese with English abstract). <https://doi.org/10.9795/bullgsj.58.261>
- Suzuki T (1983) A theoretical model for dispersion of tephra. Shimozuru D and Yokoyama I ed. *arc volcanism: physics and tectonics* 95–113. <https://pages.mtu.edu/~raman/papers2/Suzuki83.pdf>
- Suzuki T (1995) Origin of so-called volcanic-ash-soil: thickness distribution in and around Central Japan. *Bull Volcanol Soc Jpn* 40:167–176. (in Japanese with English abstract). https://doi.org/10.18940/kazan.40.3_167
- Takada A, Yamamoto T, Ishizuka Y, Nakano S (2016) *Explanatory Text of Geological Map of Fuji Volcano*. Geological Survey of Japan, AIST 56 (2nd Edition)
- Takarada S (2017) The volcanic hazards assessment support system for the online hazard assessment and risk mitigation of quaternary volcanoes in the world. *Front Earth Sci* 5:102. <https://doi.org/10.3389/feart.2017.00102>
- Tsuji T, Ikeda M, Furusawa A, Nakamura K, Ichikawa K, Yanagida M, Nishizaka N, Ohnishi K, Ohno Y (2018) High resolution record of quaternary explosive volcanism recorded in fluvio-lacustrine sediments of the Uwa basin, Southwest Japan. *Quat Int* 471:278–297. <https://doi.org/10.1016/j.quaint.2017.10.016>
- Uesawa S (2020) TephraDB_Prototype_ver1.1. <https://doi.org/10.5281/zenodo.5109160>
- Uesawa S, Nakagawa M, Umetsu A (2016) Explosive eruptive activity and temporal magmatic changes at Yotei volcano during the last 50,000 years, Southwest Hokkaido, Japan. *J Volcanol Geotherm Res* 325:27–44. <https://doi.org/10.1016/j.jvolgeores.2016.06.008>
- Wardman JB, Wilson TM, Bodger PS, Cole JW, Stewart C (2012) Potential impacts from tephra fall to electric power systems: a review and mitigation strategies. *Bull Volcanol* 74:2221–2241. <https://doi.org/10.1007/s00445-012-0664-3>
- Waythomas CF, Power JA, Richter DH, McGimsey RG (1998) Preliminary volcano-hazard assessment for Akutan volcano, east-central Aleutian Island. In: *Geological Survey Open-File Report, Alaska, U.S.A.* <http://pubs.er.usgs.gov/publication/of98360>, pp 98–360
- Wilson G, Wilson TM, Deligne NI, Cole JW (2014) Volcanic hazard impacts to critical infrastructure: a review. *J Volcanol Geotherm Res* 286:148–182. <https://doi.org/10.1016/j.jvolgeores.2014.08.030>
- Wohletz K, Heiken G (1992) *Volcanology and geothermal Energy*. University of California Press, Berkeley, p 415 <http://ark.cdlib.org/ark:/13030/ft6v19p151/>
- Yamamoto T, Nakada S (2014) In: Papale P, Shroder JF (eds) *Extreme volcanic risks 2: Mount Fuji*. In: *volcanic hazards, risks, and disasters, hazards and disasters series*. Elsevier, Amsterdam, p 505. <https://www.elsevier.com/about>
- Yamano H, Nishino H, Kurisaka K, Yamamoto T (2018) Development of probabilistic risk assessment methodology against volcanic eruption for sodium-cooled fast reactors. *ASCE-ASME J Risk Uncertain in Eng Syst B Mech Eng* 4:030902-1–030902-9. <https://doi.org/10.1115/1.4037877>
- Yang Q, Bursik M (2016) A new interpolation method to model thickness, isopachs, extent, and volume of tephra fall deposits. *Bull Volcanol* 78:68. <https://doi.org/10.1007/s00445-016-1061-0>
- Yang Q, Pitman EB, Bursik M, Jenkins S (2021) Tephra deposit inversion by coupling Tephra2 with the Metropolis-Hastings algorithm: algorithm introduction and demonstration with synthetic datasets. *J Appl. Volcanol.* 10: 1. <https://doi.org/10.1186/s13617-020-00101-4>
- Yokoyama I, Tilling RI, Scarpa R (1984) *International Mobile early-warning system (s) for volcanic eruptions and related seismic activities*, Paris; UNESCO FP/2106-82-01 2296, p 102
- Yoshimoto M, Shimano T, Nakada S, Koyama E, Tsuji H, Iida A, Kurokawa M, Okayama Y, Nonaka M, Kaneko T, Hoshizumi H, Ishizuka Y, Furukawa R, Nogami K, Onizawa S, Niihori K, Sugimoto T, Nagai M (2005) Mass estimation and characteristics of ejecta from the 2004 eruption of Asama volcano. *Bull Volcanol Soc Jpn* 50:519–533. https://doi.org/10.18940/kazan.50.6_519

Publisher's Note

Springer Nature remains neutral with regard to jurisdictional claims in published maps and institutional affiliations.